MODELLING OF HEAT TRANSFER BETWEEN TWO FUEL SUBCHANNELS IN SUPERCRITICAL WATER CONDITIONS USING COMPUTATIONAL FLUID DYNAMICS

M. Kinakin, A. Adenariwo, G.D. Harvel, and I. Pioro
Faculty of Energy Systems and Nuclear Science
University of Ontario Institute of Technology
2000 Simcoe St. North, Oshawa, Ontario, L1H 7K4 Canada
maxime.kinakin@mycampus.uoit.ca; adepoju.adenariwo@uoit.ca; glenn.harvel@uoit.ca; igor.pioro@uoit.ca

Abstract

This paper investigates the application of FLUENT in simulating a SuperCritical Water Reactor (SCWR) pressure tube type design. Computational Fluid Dynamics (CFD) can be used to study the unstable behaviour around pseudo-critical conditions along the fuel channel. In SCWRs, the coolant reaches its pseudo-critical temperature early in the reactor core and thermophysical properties undergo dramatic changes. The heat-transfer mechanism along the fuel channel also changes beyond the pseudo-critical point due to the fluid acting more like a gas-like.

The subchannels between different rings in the fuel string receive different heat fluxes and as a result, different heat transfer rates. The pseudo-critical point for different subchannels may occur at different axial locations. While experiments will be required to properly understand this effect, it is important to determine the current prediction capability of CFD type codes for this phenomenon as it will assist in defining the type of validation exercises necessary for design activities.

1. Introduction

There are a number of new concepts for nuclear reactors being developed worldwide as part of the Generation IV collaboration project. One such concept is a SuperCritical Water-cooled Reactor (SCWR), which is expected to have a thermal efficiency up to 50% [1]. SCWRs will use Super Critical Water (SCW) as a coolant, thus requiring operation at higher temperatures and pressures compared to those of current reactors. While current CANDUs and PWRs operate at a coolant pressure within 10 – 16 MPa, SCWRs will operate in the range of 25 MPa. The coolant would thus pass through the pseudocritical region somewhere along the channel [2].

Two types of SuperCritical Water-cooled Reactor (SCWR) concepts include a large Pressure Vessel (PV) Type as well as standard CANDU Pressure Tube (PT) Type Reactors. The current fuel-channel reference design for a PT Type Reactor consists of a bundle covered with a ceramic layer, enclosed by a pressure tube [3]. The outer surface of the pressure tube is in contact with the moderator, while a perforated liner protects the ceramic layer from the bundles, through which flows the primary coolant.

A typical fuel channel considered for a SCW type reactor contains a cylindrical bundle with rod type elements [4]. In such a design, the fuel bundle forms flow paths referred to as subchannels, each receiving heat from a set of 3 or 4 different cylindrical fuel elements. Optimum fuel bundle performance is affected by the design of the fuel bundle. This includes in particular heat transfer into gaps and subchannels, and the associated momentum and energy exchange between subchannels.

The subchannels between different rings of the fuel bundle have different heat fluxes, resulting in different heat-transfer rates. This configuration results in some subchannels heating faster than others. For a supercritical fluid, the pseudocritical point may occur at different axial locations along each subchannel. Changes in the fluid behaviour due to fluid-property transitions may or may not occur due to the influence of the neighbouring subchannels. Even for low pressure fluids, the physics of fluid momentum and energy exchange between subchannels is not fully understood. While experiments will be required to fully understand this effect in supercritical conditions, it is important to determine the current prediction capability of CFD-type codes for this phenomenon as this will assist in defining the type of validation exercises necessary for design activities.

In this work, two subchannels in the horizontal orientation are modelled with the FLUENT code with boundary conditions consistent with SCWR fluid conditions near the pseudocritical point at 25 MPa and 384 °C. The fluid flows parallel to the walls of the pin and heat fluxes for each fuel pin are varied around a base heat flux such that transitions through the channel would normally occur several centimetres away from each other if no influences of the neighbouring channels are considered. Computational fluid dynamics (CFD) modelling of a CANDU fuel subchannel is of particular interest at supercritical conditions to understand the heat transfer phenomena for the Gen-IV SCW CANDU design. While some work has been done in this field [9, 12], additional work is necessary. This work concentrates on modelling SCW flow in two subchannels before the pseudocritical point to determine what phenomena is predicted by the FLUENT code.

2. Model Development

The FLUENT-12 CFD code is used for this work to perform the simulations. The geometry configuration was developed with GAMBIT finite element modelling software. While the fuel bundle design for the SCWR type reactor is not yet chosen, a representative design is needed. For this work, the CANFLEX (43-element) CANDU fuel bundle design was chosen for this analysis.

Table 1 shows the properties of the CANFLEX bundle used in the analysis. The reference case is a Channel Thermal Power of 8.5 MW_{th} with uniformly distributed heat flux across the channel [4].

Table 1: Variant-20 CANFLEX-type Fuel Bundle Parameters near pseudocritical conditions [4]

Item	Value	Unit
Bundle Power	708.3	kW_{th}
Heated Length	0.481	m
Inlet Pressure	25	MPa
Coolant Inlet temperature	357	^{o}C
Coolant Mass Flux	1330	$kg(m^2/s)$
Centre Element Diameter	13.8	mm
Inner Element Diameter	13.8	mm
Intermediate Element Diameter	11.9	mm
Outer Element Diameter	11.9	mm
Centre Element Heat Flux	250	kW/m^2
Inner Element Heat Flux	250	kW/m^2
Intermediate Element Heat Flux	250	kW/m^2
Outer Element Heat Flux	250	kW/m^2

The channel contains 12 bundles arranged in series with enough spacing between each bundle to accommodate the bundle end plates. A heated bundle length of 0.481 m and a coolant mass-flow of 4.37 kg/s through the channel are chosen for this analysis. The pressure drop is not expected to change significantly along the bundle, thus a constant pressure of 25 MPa is assumed.

The inlet coolant temperature of 357 ^{o}C is chosen to match the inlet coolant bundle temperature of a previously modelled one-dimensional fuel channel design [4]. The analysed bundle is located prior to where the pseudocritical point is expected to occur in the channel. The coolant mass flux was calculated from an area ratio of the subchannel flow area and the channel flow area. A uniform base heat flux of 250 kW/m^2 is applied to each element surrounding the subchannels analysed in this model. This heat flux corresponds to a reduced power representative of the entrance region and is modelled uniform along the length.

The outer diameter of the fuel elements were measured from a Variant-20 CANFLEX fuel bundle prototype. The centre element and the elements located in the inner ring have an outside diameter of 13.8 mm while the intermediate and outer elements have an outer diameter of 11.9 mm.

2.1 Subchannel Selection

The geometry and layout for the 43 elements in a CANFLEX bundle are defined relative to the rings in the CANFLEX bundle. The radii of the inner, intermediate, and outer rings are located at distances of 16.5 mm, 34.6 mm, and 45.9 mm, respectively from the centre of the bundle. The centres of each element in each ring are located on the circumferences of their corresponding rings. The elements are equally spaced around the ring circumferences.

Figure 1 shows a Variant-20 CANFLEX-type fuel bundle schematic with the centre element (element-1) and inner elements (numbered from 2-8), intermediate elements (numbered from 9-22) and outer elements (numbered from 23-43). The subchannels, (numbered 1-70) represent the flow area of the bundle. Subchannels 8 and 23 (similar to subchannels 20 and 47 or any pair of subchannels with similar geometry) are the subchannels under study, and as such are used as reference in this paper.

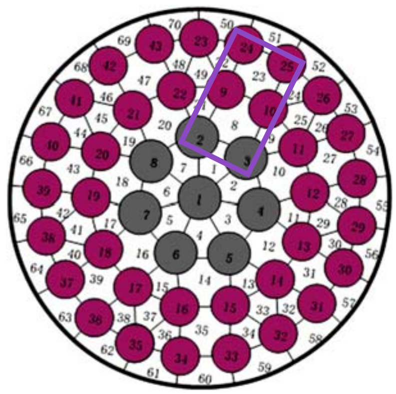

Figure 1: Schematic of Variant-20 CANFLEX-type bundle showing subchannels

Subchannels 8 and 23 receive different heat fluxes in accordance with the surrounding elements. Subchannel 8 receives heat from elements 2, 3, 9, and 10 with surrounding effects from subchannels 1, 9, 21, and 23. Subchannel 23 receives heat from elements 8, 10, 24, and 25 with surrounding effects from subchannels 8, 22, 24 and 51. The control volume selected for analysis is the union of the subchannels 8 and 23.

The subchannel selected for analysis is modelled with symmetry. The heat flux for each pin is uniform around the pin hence; the heat fluxes received by the subchannels of similar geometry are identical. The effect of the circumferential wall conduction is negligible and not taken into account since the subchannel is modelled in steady state. The flow properties are distributed as a function of the relative areas of the subchannels and therefore smaller subchannels have lower mass fluxes. This approach allows for the descritization of the model.

2.2 Mesh definition

The subchannel geometry and finite element model was generated in GAMBIT 2.4.6 software. The mesh consists of 852,480 cells axially split into 48 divisions along the length. Face meshing was first conducted before extruding the face. Boundary layers were applied to each element surface, consisting of an inflation of 1.2 with the first layer located at a distance of 5×10^{-6} m from the wall, representing the fuel element in this case. Each edge of the subchannel face was meshed with a mesh count per edge as shown in Figure 2. The numbers shown in the Figure represent the number of edge meshes for each edge. For instance element 10, of which half of the circumference is relevant in the subchannel geometry (refer to Figure 1), is divided into 160 equal spaces. Correspondingly, element 25 of which a quarter is relevant in the subchannel is divided into 80 equal spaces. The edge joining elements 10 and 25 is divided into 30 spaces which are in line with the boundary layers previously defined for both elements 10 and 25. The mesh division on this edge beyond the boundary layer of the neighbouring elements (10 and 25) is equally spaced. A mesh was then applied over the subchannel face.

The face was extruded without the mesh to 0.481m corresponding to the full heated length of 1 full bundle. An edge mesh was then applied to each axial edge of the subchannel volume before a volume mesh was generated using the hex/wedge cooper scheme option available in GAMBIT.

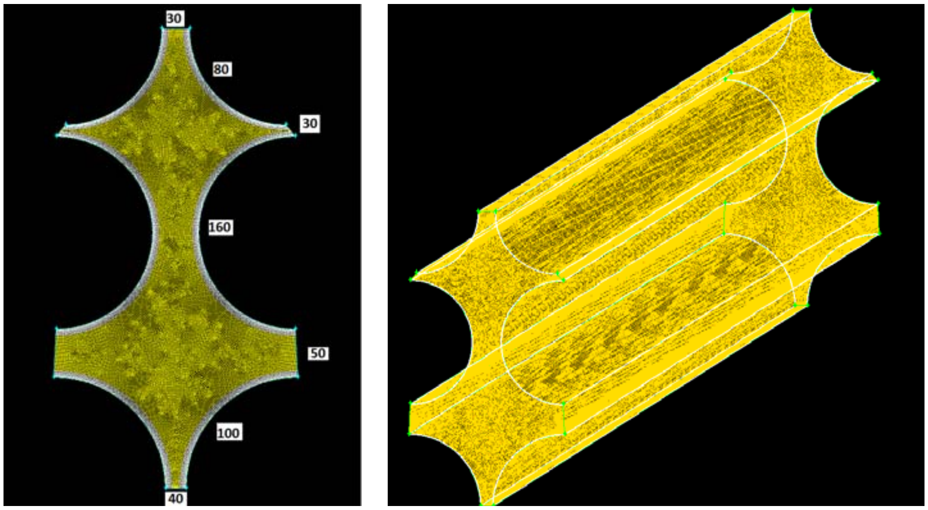

(a) Cross-sectional mesh view **(b) Isometric mesh view**

Figure 2: Subchannel mesh view; (a) Cross-sectional view (b) Isometric view

2.3 Viscous Model Selection

The k-ϵ turbulence model was adopted since it is the well known two-equation energy transport turbulence model developed by Jones and Launder [7]. The model works by conserving the energy contained within a turbulent region by means of transport equations that carry that total energy (and its dissipation) along a geometrical flow path. The variables k and ϵ represent the total turbulent kinetic energy and the dissipation rate of energy respectively. The two quantities are described as follows:

$$k = \frac{u^2+v^2+z^2}{2} \qquad \left(\frac{m^2}{s^2}\right) \tag{1}$$

Where u, v, and z represent the one-dimensional velocities of fluid contained within the three dimensional domain. The dissipative energy term ϵ, is described as follows:

$$\epsilon = \rho C_\mu \frac{k^2}{\mu_t} \qquad \left(\frac{m^2}{s^3}\right) \tag{2}$$

Where ρ is the density of the fluid, C_μ is a constant taken to be 0.09 as defined by the standard k-ϵ model. The definition of ϵ can be expressed in a compact term:

$$\epsilon = \frac{k^{3/2}}{l} \quad where \quad l = \frac{\rho C_\mu}{\mu_t \sqrt{k}} \tag{3}$$

The characteristic length scale l, represents the maximum diameter of an energy containing eddy. The k- ϵ model is the most basic and documented turbulence model being able to solve many complex flows.

2.4 FLUENT Methodology

The mesh was exported from the GAMBIT 2.4.6 software and read into FLUENT for computational flow simulation. The Realizable k-ϵ (RKE) turbulence model with an enhanced wall treatment was used to solve the mesh, including use of the thermal effects option. The RANS (Reynolds Averaging Navier Stokes) approach was used to investigate for a steady solution.

Simulation was performed using a coupled pressure-velocity solver and solutions to the transport equations were conducted using second order algorithms. Momentum and pressure relaxation factors were each set to 0.5 and energy to 0.999 to mitigate initial oscillations in the solver. Under-relaxation provides a brake on the solution, allowing for smaller initial oscillations but requiring more iterations for convergence. Neglecting to apply a relaxation may cause the iteration to oscillate beyond the temperature range defined in the REFPROP database which consequently causes FLUENT to abort the solution.

The solution was solved with an absolute convergence criterion of 10^{-5} for the each of the variables contained in the transport equation including continuity, x-, y- and z-velocity, energy, and epsilon.

The adopted boundary condition includes no-slip at the solid walls (fuel element which are the curved surfaces as shown in Figure 2). The inlet fluid temperature was set to 357°C with a turbulent intensity of 8%. The heat fluxes (refer to table 2) imposed on each element were applied as boundary conditions. Water properties at a pressure of 25MPa in the temperature range of interest were obtained from National Institute of Standards and Technology, reference Properties of database (NIST REFPROP) using a text command in FLUENT [8]. The use of NIST is essential since the fluid properties are near the region of the pseudocritical point of water. The fluid properties change considerably in a very narrow range within this region which causes the solver to become unstable.

3. Results

The results show that for the given fluxes in Table 2, initial iterations oscillated outside the range of the NIST properties database resulting in a crash of the solver. An adjustment to the input fluxes was made to eliminate this challenge.

3.1 Axial variation of coolant properties

The coolant density and temperature are uniform at the inlet but become varied with the continuous addition of heat along the subchannel. The coolant temperature and velocity increase, while the density from the inlet to the outlet decreases in accordance with the heat flux applied to the fuel elements.

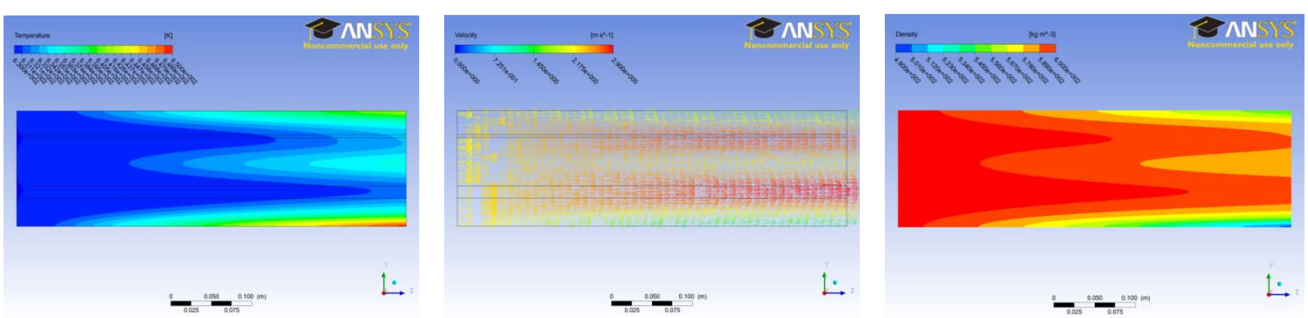

(a) Temperature contour **(b) Velocity contour** **(c) Density contour**

Figure 3: Axial Flow Variation from Inlet to Outlet; (a) Temperature contour, (b) Velocity contour and (c) Density contour

3.2 Temperature variation of coolant

A three-dimensional variation can be simulated by plotting cross-sectional temperature variations at intervals along the subchannel. This captures the details omitted by a one-dimensional model. The one-dimensional model assumes a single coolant temperature at different nodes across the fuel bundle [4].

Figure 4 shows a temperature gradient at intervals along the bundle. As expected, an increase of the temperature of the coolant is seen along the bundle. The temperature of the coolant at the narrow regions in the subchannel shows a significant increase in temperature along the subchannel than the coolant region far from the wall.

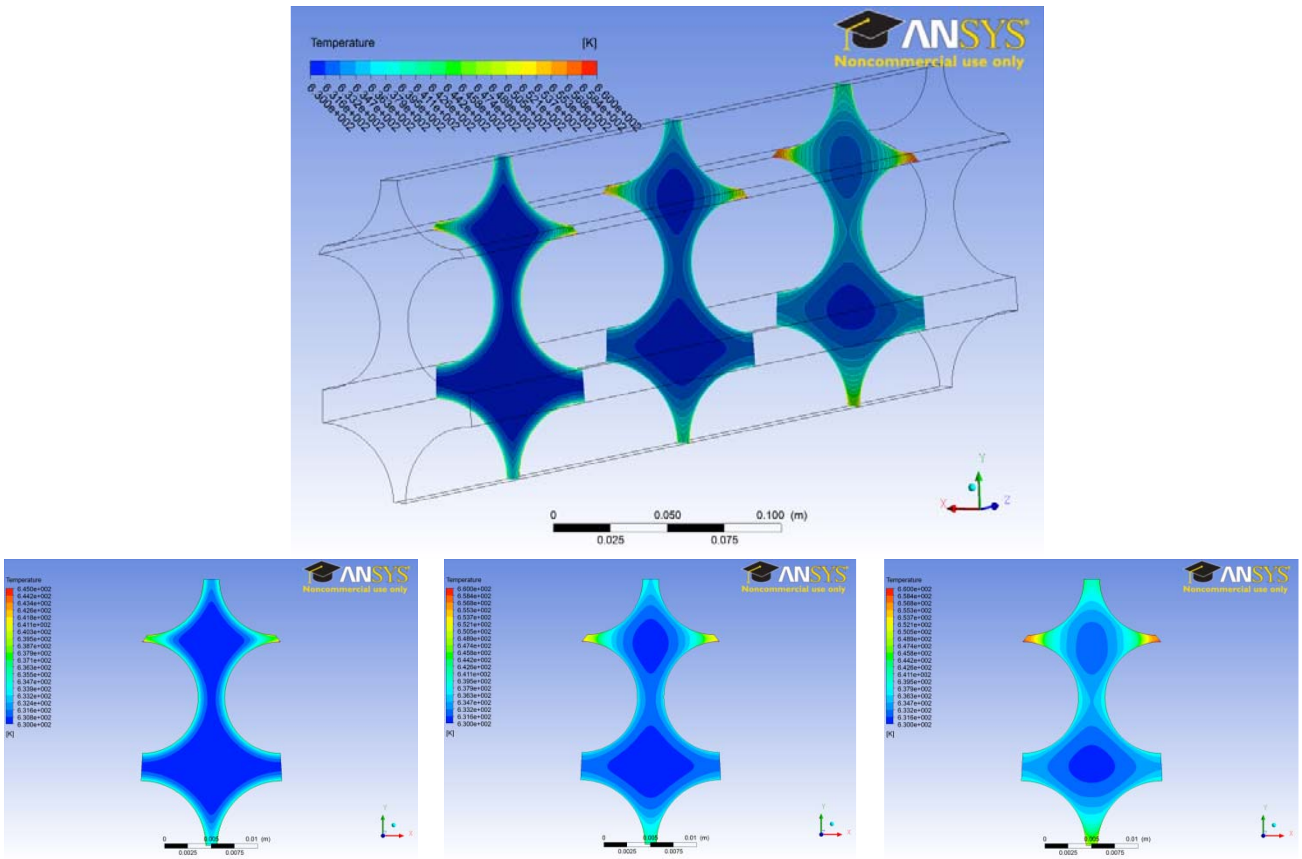

(a) z = 0.1 m **(b) z = 0.25 m** **(c) z = 0.4 m**

Figure 4: Axial cross-sectional temperature variation at a distance (z) from subchannel inlet; (a) z = 0.1 m, (b) z = 0.25 m and (c) z = 0.4 m

The fluid is essentially unheated at z = 0.1 m but the narrow region of the coolant shows a 25^{o}C difference in temperature with the coolant region farthest from the wall. At z = 0.25 m, a temperature gradient is observed across the fluid moving from the wall to the centre of the subchannel. The coolant between the narrow spacing between elements 25 and 10, and 24 and 9 (refer to Figure 1) maintains the highest fluid temperature in the subchannel. The top and bottom spaces between elements 24 and 15, and 2 and 3 respectively begin to significantly heat up at this point. At z = 0.4 m, the temperature gradient shows a more even variation with a 30^{o}C temperature difference between the narrow spacing and the centre of the subchannel. The coolant in the upper subchannel shows a more varied temperature profile than the coolant in the lower subchannel.

The reason for the high temperature regions across the cross-sectional can be explained by low coolant velocity. Low coolant velocity means low heat transport properties which in turn causes heat to build up close to the wall of the element in the narrow region. The narrow spacing between the elements contains the fluid with the highest temperature which subsequently means pseudocritical phenomena will first occur at this region.

3.3 Velocity variation of coolant

The velocity profile at is plotted at the same intervals as the temperature profiles. The low velocity regions are located close to the wall as expected from the no-slip boundary condition. The coolant region farthest from the wall at the inlet has a maximum velocity of 2.9 m/s. The velocity distribution becomes more uniform along the channel with a decrease of the average velocity. This decrease of the velocity becomes less significant from z = 0.25 m to z = 0.4 m when compared to the change from z = 0.1 m to z = 0.25 m. This suggest that the flow is developing from z = 0.1 m to z = 0.25 m and is almost fully developed between z = 0.25 m to z = 0.4 m.

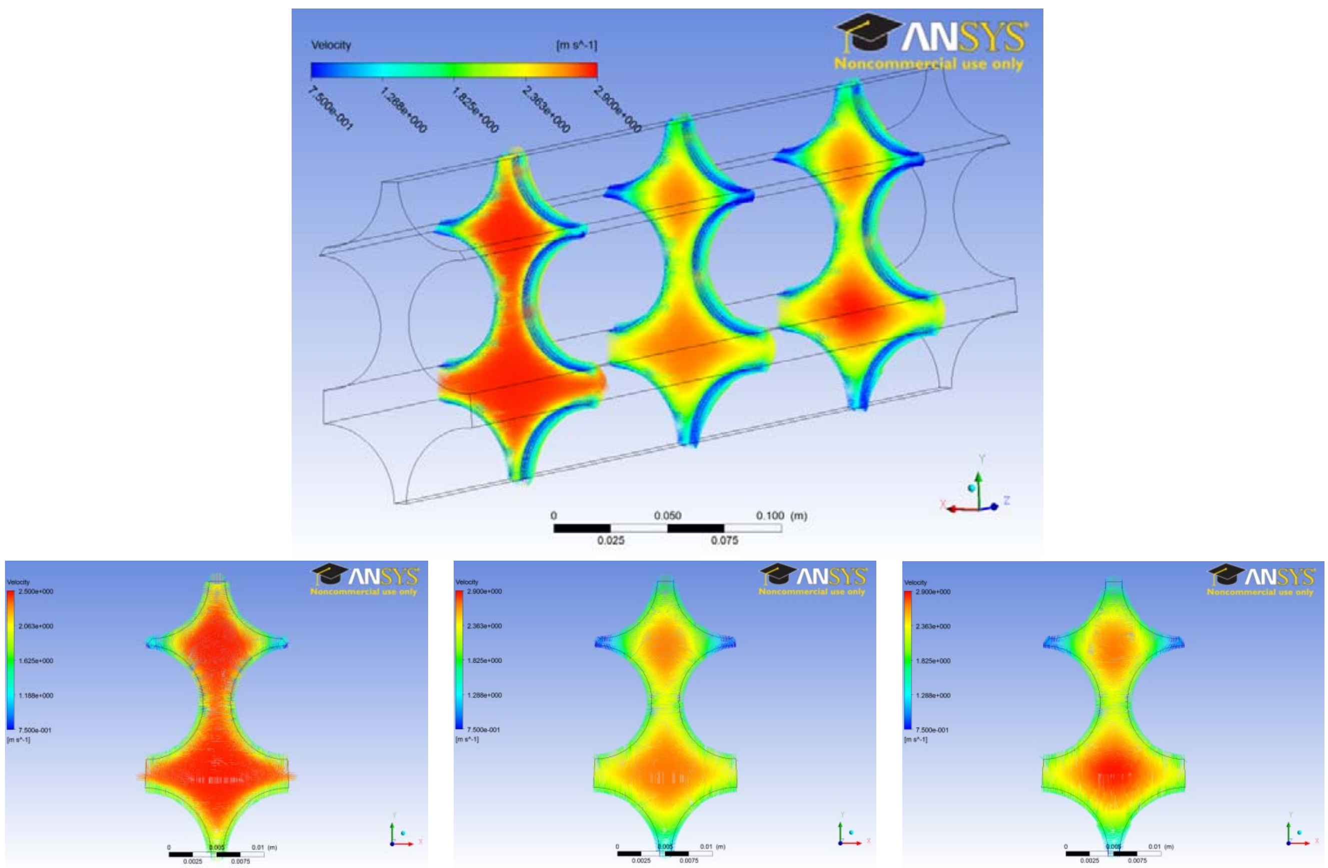

(a) z = 0.1 m **(b) z = 0.25 m** **(c) z = 0.4 m**

Figure 5: Axial cross-sectional velocity variation at a distance (z) from subchannel inlet; (a) z = 0.1m, (b) z = 0.25 m and (c) z = 0.4 m

The coolant region with low velocity is located at the narrow regions of the subchannel. The upper subchannel has a more pronounced effect of low velocity than the lower subchannel. The profile at z = 0.4 m, shows a larger area with coolant velocity close to maximum flow velocity. This is expected as the lower subchannel has a higher flow area than the upper subchannel. The effect of the no-slip boundary on the wall is less evident at the centre of the lower subchannel.

3.4 Density variation of coolant

The coolant density across the subchannel decreases from the inlet to the outlet. At a distance of z = 0.1 m downstream from the inlet, the coolant density is uniform at 620 kg.m^{-3} across the subchannel. The bulk density is close to 590 kg.m^{-3} at a distance of z = 0.4 m downstream from the inlet and in the subchannel region with narrow spacing, the value is close to 480kg.m^{-3}.

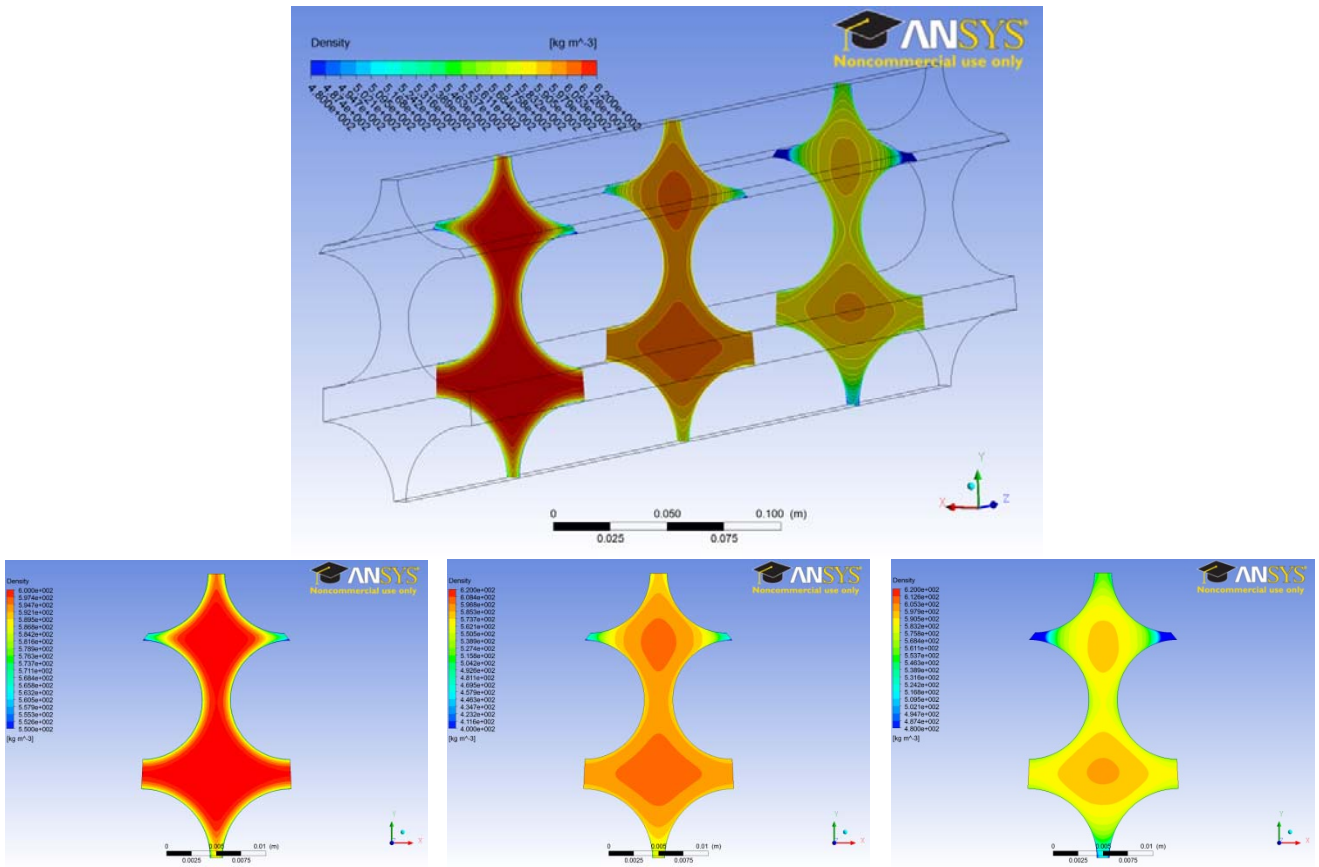

(a) z = 0.1m (b) z = 0.25m (c) z = 0.4m

Figure 6: Axial cross-sectional density variation at a distance (z) from subchannel inlet; (a) z = 0.1m, (b) z = 0.25m and (c) z = 0.4m

As the coolant heats up along the subchannel, the density decreases with minimum values located at the narrow spacing located in the upper subchannel. A low density region is located in the lower region of the lower subchannel. The coolant in the upper region of the upper subchannel has higher density compared to the lower region of the lower subchannel due to the better heat transport properties. The low density regions result from high heat transfer coupled with low fluid velocity in the region. The results show the expected change in properties across the subchannel.

4. Conclusion

A CFD analysis was performed for a selected subchannel in a Variant-20 CANFLEX-type bundle. A constant heat flux was applied to the elements surrounding the subchannel and temperature, velocity and density gradients were obtained at different positions along the bundle. The variations show that the pseudocritical point will first occur at the narrow regions close to the wall.

While work has been done on a reference subchannel, it would be useful to compare the variation of properties independently for the subchannels contained in the reference subchannel. Varying the base heat flux boundary condition will be useful for simulating a more representative model for the fuel bundle. An improvement to the model will include redefining the mesh to reduce extreme variations seen at the narrow regions in the subchannel, as well as to allow fluid flow to completely develop before the heated length of the bundle. Mesh refinement can be performed to obtain a higher order of convergence. The RANS approach gives a convergence of 10^{-5}. An unsteady solution may yield better convergence for the model and will be investigated in future work.

5. References

[1] M. Naidin, S. Mokry, and I. L. Pioro, “SCW NPPs: Layouts and Thermodynamic Cycles”, Proceedings of Nuclear Energy for New Europe, Bled, Slovenia, 2009 Sep 14 – 17.

[2] I. L. Pioro and R. B. Duffey, “Heat Transfer and Hydraulic Resistance at Supercritical Pressures in Power Engineering Applications”, ASME Press, New York, NY, USA, 2007. pp. 1-334.

[3] C. K. Chow and H. F. Khartabil, “Conceptual Fuel Channel Designs for CANDU – SCWR”, Nuclear Engineering and Technology, 2008, pp. 1-8.

[4] J. Samuel, G.D. Harvel, and I. Pioro, “Design Concept and Heat Transfer Analysis for A Double Pipe Channel for SCWR Type Rectors”, Proceedings of the International Conference on Nuclear Engineering (ICONE-18), Xi’an, China, 2010, May 17-21.

[5] M. Sharabi, W. Ambrosini, S. He, Pei-xue Jiang, Chen-ru Zhao, “Transient 3D Stability Analysis of SCWR Rod Bundle Subchannels By a CFD Code”, Proceedings of the International Conference on Nuclear Engineering (ICONE-16), Orlando, Florida, USA, 2008. May 11-15.

[6] Y. Jiyang, W. Songtao, J. Baoshan, “Developement of sub-channel analysis code for CANDU-SCWR”, Progress in Nuclear Energy, Beijing, China, 2007. pp. 334-350.

[7] B. E. Launder and W.P. Jones, “The Calculation of Low Reynolds Number Phenomena with a Two-Equatio Model of Turbulence”, Heat and Mass Transfer, vol. 16, no. 6, pp. 1119-1130, 2973.

[8] National Institute of Standards and Technology, “NIST Reference Fluid Thermodynamic Transport Properties – REFPROP,” NIST Standard Reference Database 23, Ver. 8.0, vol. Boulder, CO. US Department of Commerce.

[9] G. Hazi and I. Farkas, “On the Pressure Dependency of Physical Parameters in Case of Heat Transfer Problems of SCW”, Proceedings of the International Conference on Nuclear Engineering (ICONE-16), Orlando, Florida, USA, 2008. May 11-15.

[10] K. e. a. Kuehlert, "Fluid-Structure Interaction of a Steam Generator Tube in a Cross-Flow Using Large-Eddy Simulation", Proceedings of the International Conference on Nuclear Engineering (ICONE-14), Miami, USA, 2006. July 17-20.

[11] A. Muhana and D.R. Novog, "Validation of FLUENT for Prediction of Flow Distribution and Pressure Gradients in a Multi-Branch Header Under Low Flow Condition", Proceedings of the International Conference on Nuclear Engineering (ICONE-16), Orlando, Florida, USA, 2008. May 11-15.

[12] D. Wilcox, "Simulation of Transition with a Two-Equation Turbulence Model", AIAA Journal, 1994. vol. 32, no.2, pp. 247-255.